ERYTHROCYTE AND GHOST CYTOPLASMIC RESISTIVITY AND VOLTAGE-DEPENDENT APPARENT SIZE

STEPHEN P. AKESON AND HOWARD C. MEL
Department of Biophysics and Medical Physics, University of California, Berkeley California 94720

ABSTRACT Particle resistivity is explicitly included in the equations relating volume to voltage pulse, in electronic cell sizing or resistive pulse spectroscopy (RPS). It has long been known that in high electric fields cell resistivity decreases as the membrane undergoes dielectric breakdown. At sufficiently high electric field strengths, well past dielectric breakdown, the red cell membrane becomes electrically transparent, or nearly so, and apparent cell size becomes essentially a function of the cytoplasmic resistivity. Electronic cell sizing is traditionally carried out at low electric field strengths, and corrections made for the influence of cell shape by use of the Laplace equation. We find the Laplace solution to be still applicable at very high electric field strengths for purposes of calculating specific cytoplasmic resistivity from RPS measurements. Our value for discocytes, 220 Ω·cm, is in good agreement with published results obtained by other researchers using other techniques. We have also applied these same procedures to determine the time course of voltage-dependent resistivity changes in ghosts and intact spherocytes, during the first 5 min after suspension in hypotonic medium. We believe these to be the first explicit calculations of particle specific resistivity from post–dielectric-breakdown apparent size, using traditional electronic sizing techniques.

INTRODUCTION

Electronic cell sizing, as introduced by Coulter (1956), started out by assuming that the membrane was a sufficiently good insulator that the ratio of medium resistivity to particle resistivity was effectively zero. Experimental evidence of the need for a more complex sizing theory was found as early as 1962 (Brecher et al.), when it was noted that high aperture currents led to abnormally small apparent size. Zimmermann et al. (1974) showed that the small apparent size seen at high electric fields resulted from dielectric breakdown of the cell membrane.

Much of the theory of electrical properties of cells in suspension was tested in parallel plate discharge experiments, where the electric fields are relatively homogeneous. It was found that many types of cells would lyse in such experiments if the applied fields were very high. While studying electrical lysis, Sale and Hamilton (1968) concluded that the effect was due to an induced membrane potential, and noted that there seemed to be a threshold of ~1 V in this potential for lysis to occur. Zimmermann et al. (1976*a*) and Kinosita and Tsong (1977*a,b,c*) confirmed this and showed that the basis of electrical hemolysis was the disruption of ion permeability barriers by dielectric breakdown of the cell membrane, leading to subsequent colloidal osmotic hemolysis.

Believing the postbreakdown electric field and membrane resistance to be spatially inhomogeneous, Jelish and Zimmermann (1979) rejected the Laplace solution to the problem of particle resistivity, and modeled the process empirically. Their work produced a method for accurate detection of dielectric breakdown during cell sizing, and a procedure for measurement of particle resistivity, based on the slope of the curve for change in signal vs. change in applied field. A sizing apparatus using a voltage ramp was designed to make such measurments, as described by Groves (1980), and as patented by Zimmermann et al. (1980*a,b*).

We present evidence herein that, from a practical point of view, the Laplace equation can still be usefully applied for certain purposes, namely for calculation of internal resistance at very high electric fields. Based on the approximation of a negligible membrane resistance at very high electric fields, we have calculated the cytoplasmic resistivity of erythrocytes, and compared the results with those obtained by Pauly and Schwann (1966) using dielectric dispersion methods. Calculations and comparisons were also made for the high electric field resistivities in osmotically swollen spherocytes.

The Laplace solution was then applied to determine the changes in cytoplasmic resistivity of ghosts and intact cells during the first 5 min after suspension in hypotonic media, and the results interpreted in terms of a recently proposed model of hemolysis (Akeson and Mel, 1982). We also demonstrated a new phenomenon in the electronic sizing of ghosts, where interaction with sufficiently high electric fields rendered ghosts completely transparent to the sizing process, so that the ghosts effectively "disappeared."

MATERIALS AND METHODS

Suspending and Sizing Media

The basic medium used in all experiments was Dulbecco's phosphate-buffered saline (PBS) (in milligrams per liter: 100 $CaCl_2$, 200 KCl, 200

KH_2PO_4, 100 $MgCl_2 \cdot 6\,H_2O$, 8,000 NaCl, 2,170 $Na_2HPO_4 \cdot 7\,H_2O$. Slight adjustments were made to 300 mOsM, at pH 7.3, by adding small amounts of NaCl, H_2O, HCl, or NaOH, as appropriate). Hypotonic solutions were made by dilution of isotonic PBS with deionized water. Osmolalities were measured using a Wescor Inc. (Logan, UT) 5100B vapor-pressure osmometer.

Sample Preparation

Blood samples were obtained from apparently healthy humans by finger prick. A primary dilution, consisting of two drops of whole blood in 10 ml of PBS, was incubated at room temperature for 30 min, to avoid transients in osmotic properties (Mel and Reed, 1981). Subsequent sizing experiments were done on secondary, 1:100 dilutions from this stock. For kinetic studies, the secondary dilution was made at time zero, and the computer was used to collect and store sequential apparent-size spectra every 5 s for 5 min.

Resistive Pulse Spectroscopy (RPS)

The apparatus for resistive pulse spectroscopy (RPS) has already been described by Yee and Mel (1978*a*). For this work, measurements were made using a 48 × 48 μm (diameter × length) cylindrical bore orifice, without hydrodynamic focusing. To avoid complications from deformability effects (Yee and Mel, 1978*b*), all measurements were taken at slow flow (0.002 ml/s, corresponding to a pressure drop across the orifice of 1.5 cmHg). All measurements were made at room temperature, 22° ± 1°C.

The orifice-manometer system is from Particle Data, Inc. (Elmhurst, IL), the electronics and software were of our own design, and the PDP 8/I computer system used for digitalization, data collection, and analyses of resistive pulses and their spectra was from Digitial Equipment Corp. (Maynard, MA).

Cell Sizing Theory

An excellent review of the theory of electrical sizing is given by Kachel (1979). The specific equations that follow are derived in Akeson (1982). The basic approach in electronic cell sizing is the application of a constant current, i, through a small diameter orifice, and subsequent measurement of the change in potential across the orifice, ΔU, necessary to maintain the constancy of current during the passage of a particle. The fundamental equation relating particle volume, ΔV, to the voltage pulse, ΔU, is

$$\Delta U = \frac{\Delta V}{V} \cdot \rho_{med} \cdot \frac{L'}{Q} \cdot f_E \cdot i. \tag{1}$$

Here V is the volume of the orifice, ρ_{med} is the specific resisitivity of the medium, L' and Q are the electrical length and cross-sectional area of the orifice, and f_E is a combined shape and conductivity factor, reflecting the influence of the geometrical properties of the particle on the electric field in the orifice. When a zero-input-impedance amplifier is used to amplify ΔU, the gain g_{amp} is equal to $-R_f/(\rho_{med} \cdot L'/Q)$, where R_f is the feedback resistance. The output from the amplifier is then

$$\Delta U \cdot g_{amp} = \frac{-\Delta V}{V} \cdot R_f \cdot f_E \cdot i$$

$$= \frac{-R_f \cdot i}{V} \cdot \Delta V \cdot f_E. \tag{2}$$

Using such an amplifier makes the resistive pulse height independent of ρ_{med}. Except for possible second-order effects, the relationship between the measured signal, ΔU. g_{amp}, and the apparent size, $\Delta V \cdot f_E$, is linear.

In practice, the measured volume is a peak channel from a pulse height analyzer. Eq. 2 can thus be restated as

$$\Delta V \text{ (measured channel No.)} = C \cdot \Delta V \text{ (cubic micrometers)} \cdot f_E. \tag{3}$$

To evaluate the constant C, which relates channel number to volume, we have calibrated with 5.9 μm (nominal) diam polystyrene microspheres (Duke Scientific Corp., Palo Alto, CA) that have $f_E = 1.5$ (Grover, 1969).

The critical problem, and subject of this paper, is the evaluation of the shape and conductivity factor, f_E, for membrane-bounded particles such as red cells. As originally proposed by Sale and Hamilton (1968), if the membrane is sufficiently thin compared with the cell diameter, then the particle can be treated as homogeneous. Following Kachel (1979), we define f_E as

$$f_E = \frac{2\left(1 - \frac{\rho_{med}}{\rho_{part}}\right)}{2 + ab^2L_a\left(\frac{\rho_{med}}{\rho_{part}} - 1\right)}. \tag{4}$$

This solution is exact, in the case where the particle is electrically homogeneous. The quantity ab^2L_a is a dimensionless number reflecting the Laplace solution for the influence of particle shape and orientation on the electric field. For ellipsoids of revolution, Velick and Gorin (1940) have tabulated the values of ab^2L_a; they range from 2/3 for spheres to 1/3 for disks (oblate ellipsoids) similar in shape to native red blood cells.

The quantity of interest is ρ_{part}, the specific resistivity of the particle. Assuming that the true particle volume, ΔV, is constant (and keeping the product $R_f \cdot i$ constant), Eq. 2 states that all variation in measured size as a function of electric field strength is due to changes in f_E. In f_E there are two variable quantities: ab^2L_a, and ρ_{part} (Eq. 4). In contrast to Jelish and Zimmermann (1979), we have assumed that ab^2L_a is the same for both low and high fields, and solved for ρ_{part}. By making calibrated measurements at low voltages, and using the accepted nonconducting shape factors, we obtain values for ΔV. These are then used to solve for f_E, and then ρ_{part}, in the high electric field state.

Electric Field Variation

The electric field strength within the orifice was varied in two ways. Our constant current source had a typical geometrical doubling pattern. To obtain data from intermediate field strengths, we also varied the solution resistivities, by dilution with 0, 10, 20, 30, 40, and 50% vol/vol solutions of isotonic sucrose in PBS. Electric field strengths were calculated from Ohm's law, using conductivities measured with a Beckman Instruments, Inc. (Cedar Grove, NJ) RC-16C conductivity bridge. The voltage drop across the orifice was continuously monitored with a voltmeter, to detect clogging or heating effects. In addition, the output from the zero-input impedance amplifier was monitored continuously on an oscilloscope.

RESULTS

Fig. 1 depicts the electric field strength dependence of red blood cell apparent size, measured in a series of 300 mOsM solutions of decreasing ionic strength. While all the curves converge below ~1 kV/cm, they spread out at high field strengths, in a set of nonintersecting trajectories. Using the oblate discoid constant value of 1/3 for ab^2L_a, we have converted the apparent-size data of the discocytes of Fig. 1 into particle specific resistivities, as a function of the electric field strength in the orifice (lower curve in Fig. 2).

To test our theories on red cells in a somewhat different state, we chose to measure sphered red cells at 160 mOsM, which is just above the threshold for abrupt osmotic hemolysis (<150 mOsM). The values for spherocyte resistivity (upper curve in Fig. 2) were derived using the same mathematical relationships as for the discocytes, from measurements similar to those shown in Fig. 1. However,

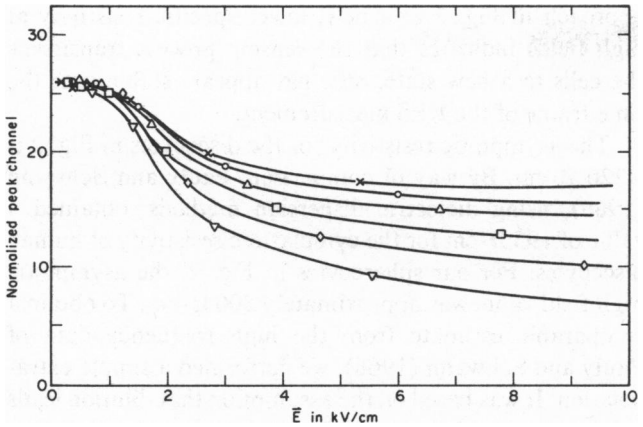

FIGURE 1 Apparent size of red cells vs. electric field strength, in 5 different vol/vol admixtures of 300 mOsM PBS with 300 mOsM sucrose. ×, O%; ○, 10%; △, 20%; □, 30%; ◇, 40%; ▽, 50% sucrose.

the cells were sized in 160 mOsM PBS/sucrose admixtures instead of 300 mOsM (primary data on apparent size not shown), where ab^2L_n is 2/3, and the nonconducting shape factor is 1.5.

In Fig. 3 are shown the kinetics of apparent size, for ghosts and intact spherocytes, at selected times during the first 5 min following suspension in 100 and 160 mOsM PBS, respectively. The two uppermost curves are for the lowest electric field strengths, while the two lower curves are the results obtained at high field strengths.

When these data were transformed into post–dielectric-breakdown particle resistivities, Fig. 4, the earliest ghost resistivity we measured was seen to be greater than that for the intact spherocytes. However, ghost resistivity fell very quickly, and by 60 s it had leveled out at a much lower value. It should be pointed out that this final resistivity (240 Ω·cm) was still significantly greater than that of the lysing medium (170 Ω·cm).

In processing the data from Fig. 3 with the resistivity algorithm, we have assumed that both the intact cells and

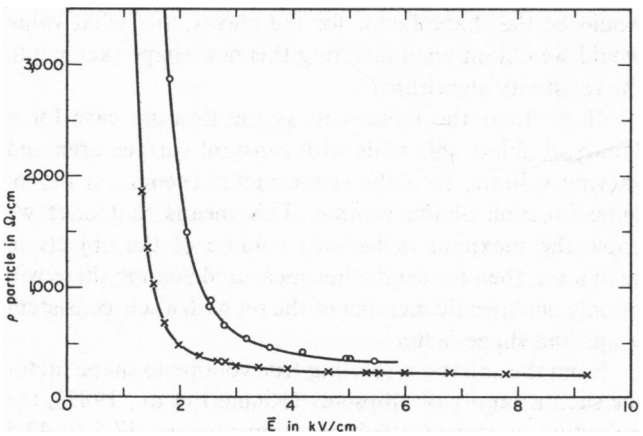

FIGURE 2 Red cell specific resistivities (calculated from apparent size) vs. electric field strength. ×, discocytes, 300 mOsM PBS; ○, spherocytes, 160 mOsM PBS.

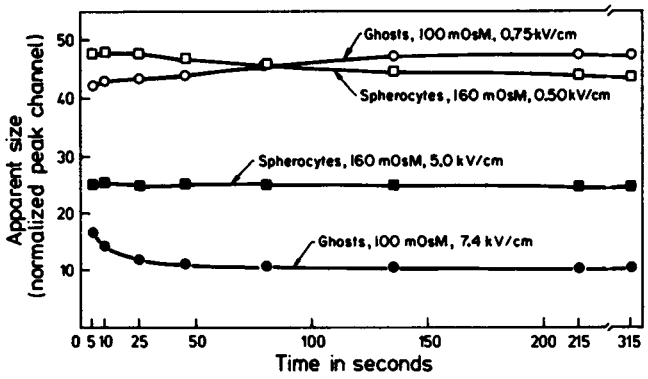

FIGURE 3 Apparent-size kinetics of ghosts and spherocytes, during the first 5 min following suspension in hypotonic PBS. Open symbols (○, □), low electric field strengths; solid symbols (●, ■), high field strengths. (Top two curves are adapted from Akeson and Mel, 1982.)

ghosts are spheres with shape factors of 1.5 in the nonconducting state, even though the apparent volume of the early ghosts was significantly smaller in the earliest time points (channel 42.5 compared with 47.5 for the intact cells). A justification for the use of 1.5 as our ghost shape factor is given in the Discussion.

In Fig. 3 we simply plotted the peaks from the ghost and intact cell (spherocyte) apparent-size spectra. While making the high-field measurements on ghosts, we noticed that the integrals for our 5-s counting periods were continuously decreasing over time, even though the peak (modal) volumes remained constant. This loss of counts, which we refer to somewhat whimsically as "the disappearing ghosts," is demonstrated in Fig. 5. To verify that the concentration of ghosts in the sizing suspension in fact remained constant, the two higher electric field measurements were made on the same sample, during a single kinetic run, switching the current setting back and forth. We were thus able to establish that most of the population

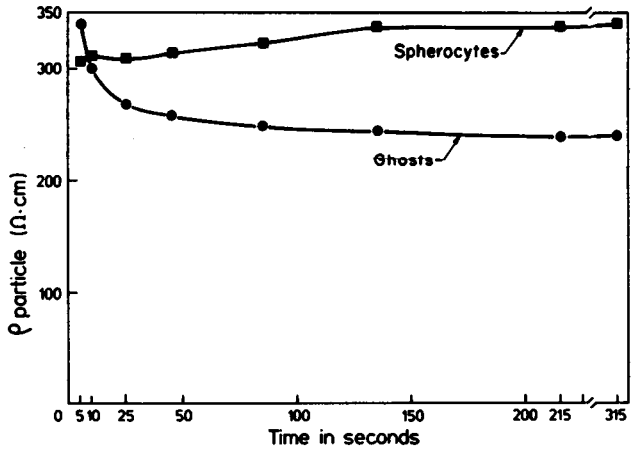

FIGURE 4 Kinetics of specific resistivity, for ghosts and intact cells at high fields, calculated using differences between apparent sizes, as measured at low and high electric fields. Ghosts in 100 mOsM, ●; Spherocytes in 160 mOsM, ■.

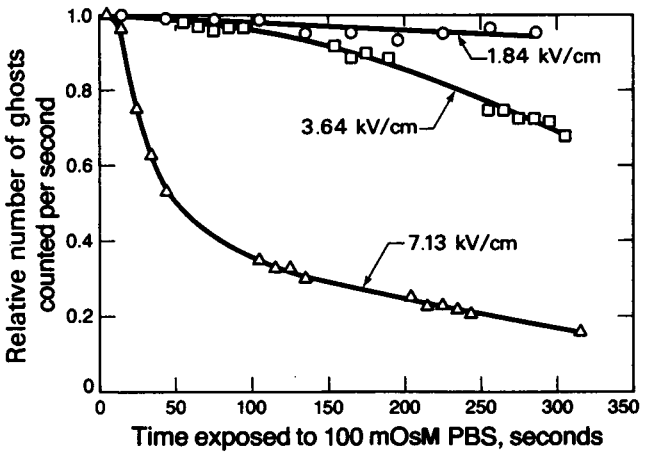

FIGURE 5 Disappearance of ghosts at high electric field strengths. Electric field strength as marked. The 3.64 kV/cm and 7.13 kV/cm measurements were taken from the same sample series.

of ghosts that was disappearing at 7.13 kV/cm was still present at 3.64 kV/cm.

DISCUSSION

Kachel (1976) was the first to use RPS-type techniques to determine particle resistivity. Although he used very high electric field strengths, he chose to make measurements only on latex spheres and glutaraldehyde-fixed red cells. Neither of these has any voltage-dependent resistance, at least within the range of field strengths (and for the 0.5% glutaraldehyde concentration) he used. Other work in our own laboratory confirms this conclusion.

This is not the case for native red blood cells; the apparent size of such cells is a very nonlinear function of the applied field strength, as shown in Fig. 1. In our analysis, we began by assuming that the low electric field, apparent-size plateau reflected the true volume of an infinitely resisitive cell. We then treated all reductions in apparent size at high field strengths as reflections of reduced particle resistivity. As the "infinitely" resistive membrane began to conduct, the resulting current became limited, instead, by the cytoplasmic resistivity (Jelish and Zimmermann, 1979).

The transformation from the many separate curves of Fig. 1 to the single, lower curve of Fig. 2 provides an elegant demonstration of the self-consistent nature and underlying unity of the theory of electronic sizing. At first it may seem suprising that the high field strengths did not simply destroy the cells, and thereby preclude our making such measurements, considering the previous findings by Zimmermann and others that dielectric breakdown of red cells leads to hemolysis (Kinosita and Tsong 1977*a,b,c*, 1979; Zimmermann et al., 1974,1976*a,b*). Destruction was undoubtably the ultimate fate of our high electric field cells, as well. However, in RPS, the cells are analyzed concurrently with the exposure to the high electric field, before this destruction can occur. The asymptotic approach in Fig. 2 to a new, lower specific resistivity at high fields indicates that the sensing process transforms the cells to a new state, one that appears stable over the time frame of the RPS measurement.

The asymptotic resistivity for the discocytes in Fig. 2 is ~220 Ω·cm. By way of comparison, Pauly and Schwann (1966), using dielectric dispersion methods, obtained a value of 195 Ω·cm for the cytoplasmic resistivity of human discocytes. For our spherocytes in Fig. 2, the asymptotic high field value was approximately 300 Ω·cm. To obtain a comparable estimate from the high frequency data of Pauly and Schwann (1966), we performed a simple extrapolation. It was based on the assumption that dilution leads to a proportional increase of cytoplasmic resistivity. Our spherocytes were swollen to an average volume of ~120 cubic μm (data not shown); thus their expected cytoplasmic resistivity would be 120/90 × 195, or 260 Ω·cm, according to proportional dilution.

Pauly and Schwann's resistivities (measured and extrapolated) are 25 and 40 Ω·cm lower than our own, respective, experimental values. The differences may reflect one or more of the following factors: (*a*) residual or inhomogeneous membrane resistance, (*b*) deviations from our assumed shape factors, or (*c*) the limits of experimental error. In any case, the agreement is sufficiently good to propose that at least 85–90% of our high electric field resistivities can be ascribed to the internal cytoplasm.

Ghost Sphericity and Shape Factor Considerations

In arriving at the results of Fig. 4 from the data of Fig. 3, we assumed a spherical shape factor of 1.5 for the ghosts. Because the early ghost apparent volumes were actually somewhat smaller than those for the intact spherocyte (Fig. 3), this assumption cannot be rigorously valid. A more precise approach would have been to treat the ghosts as oblate spheroids, with the same surface area as for the intact cells but having a reduced volume. What, then, would be the shape factor for the ghosts, and what value would we obtain upon inserting this new shape factor into the resistivity algorithm?

If we treat the intact cell as the limiting case for a family of oblate spheroids with constant surface area and varying volume, then the shape factor becomes a monotonic function of the volume. This means that once we know the maximal (spherical) volume of the objects in such a set, then for each other measured volume there will be only one specific member of the set with a self-consistent shape and shape factor.

From the equations relating true volume to shape factor for such a family of ellipsoids (Richieri et al., 1983), the reduction in apparent volume from channel 47.5 to 42.5 implies that the earliest ghost, taken as an oblate spheroid, would have a shape factor of 1.395 and a volume equal to 0.962 of maximum volume. This corresponds to a value of

0.566 for ab^2L_a, and leads to a revision of the initial ghost resistivity from 340 ohm·cm to 325 ohm·cm. This difference (<5%) is statistically significant, but it is small enough not to change the general conclusions drawn from our data. We have therefore treated these ghosts as spheres having a shape factor of 1.5 for the remainder of this paper.

Kinetics of Resistivity Change During Osmotic Hemolysis

From our analysis of Fig. 2, we concluded that 5.0 kV/cm was sufficient electric field strength to render the membrane effectively transparent, in an electrical sense. We then used this conclusion to design an experiment to measure the kinetics of cytoplasmic resistivity changes during osmotic hemolysis. The basic data, shown in Fig. 3, consisted of two pairs of sizing series. For each cell type (ghosts, or swollen, intact cells), the kinetics of size change were measured at both low ("infinite" membrane resistance) and high ("zero" membrane resistance) electric field strengths.

The resulting kinetics of resistivity change, shown in Fig. 4, were consistent with previously published models of hemolysis (Akeson and Mel, 1982). The intact cells (cytoplasms) slowly increased in resistivity. From the work of MacGregor and Tobias (1972), we know that the cells are losing K^+ under these 160 mOsM conditions. In the first instance, this resulted in a general dehydration and shrinkage (Fig. 3). However, Fig. 4 suggests that at the same time, the proportion of current-carrying species, relative to the total osmotically active species within the cell, must have been decreasing, since there was a net increase in the cytoplasmic resistivity.

Now, turning to the process of ghost formation, the kinetics of change in resistivity were governed by the exchange of total cell contents, as opposed to a selective K^+ loss. As was recently emphasized (Akeson and Mel, 1982), the resistivity of the intact cell is substantially higher than that of the medium. Consequently, the exchange of cytoplasm with the medium during ghost formation actually led to a reduction of internal resistivity. We can view the curves of Fig. 4 as evidencing two stages to the drop in (emerging) ghost resistivity. The first was quite rapid and essentially complete by 1 min, while the second was much slower. When one considers that hemoglobin release should be part of the generalized exchange of cytoplasm with the external medium, it is not surprising that our kinetics of ghost resistivity change paralleled, exactly, the two-stage kinetics of hemoglobin release reported by Anderson and Lovrien (1977).

As was noted in Results, in confirmation of previous work (Akeson and Mel, 1982), the long-term ghost resistivity remained higher than that of the lysing medium. The likely explanation for this result was found in the ghost's residual hemoglobin: as much as 7% of the cell's original hemoglobin can be permanently trapped in the "pink" ghosts that are formed in these intermediate osmolalities (Dodge et al., 1963).

Stability of the Cell During the Sensing Process

One of the assumptions we have used in these calculations is that not only does the cell remain intact during the time of the electrical sensing process, but that its volume remains constant. From the point of view of the cell, its electrical interaction with the sensing orifice begans with the induction of an excess membrane potential, brought about by the increasing electric field occurring during the cell's approach to the orifice. Kinosita and Tsong (1977*a*) calculated that the time constant for this membrane charging process is on the order of 0.1 μs. Because we measured the rise time for the resistive pulse to be ~10 μs, this meant that throughout the sensing process, the cell's induced potential was able to remain electrically in equilibrium with the field in its immediate environment.

Once the critical membrane potential is exceeded, dielectric breakdown takes place, and one or more "pores" are formed in the membrane (Kinosita and Tsong, 1977*a,b*). This pore formation is also a rapid process, and is essentially independent of voltage-pulse duration, for pulses longer than ~1 μs (Kinosita and Tsong, 1977*a*). Because the typical pulse widths (transit times) in the present slow-flow measurements were on the order of 100 μs, we concluded that, as a worst case, when dielectric breakdown took place, it did so early in the sensing process. The question then became, If the cells were undergoing dielectric breakdown, and pores were forming in the membrane, were there significant ion fluxes (and associated volume changes) within the time frame of the measurement? (At faster flow rates, and/or lower field strengths, the magnitude of such effects, if they occurred at all, would be reduced.)

The early research on dielectric breakdown in red cells was focused in precisely this area of induced ion fluxes. High-field pulses were used to make pores in the membrane; these subsequently led to dissipation of the gradients of the small ionic species, thence to colloidal osmotic pressure induced hemolysis (Zimmermann et al., 1974,1976*a,b*; Kinosita and Tsong, 1977*a,b,c*). The limiting factor for this phenomenon was shown to be the rates of ion diffusion through the pores. Kinosita and Tsong (1977*b*) measured the initial rate of swelling after high-voltage pulsing, and found that it never exceeded 20 μm^3/min. This is so slow that during a typical 100 μs pulse, the cell has time to swell only a fraction of a cubic micrometer; i.e., the assumption of constant volume appears well justified.

Biologically Significant Fields and Disappearing Ghosts

In spite of the above discussion, the fact remains that there can be a significant alteration of the cells by the electric

field, as evidenced by the "disappearing ghosts" (Fig. 5). We believe that the key to this phenomenon probably lies in interactions that extend far beyond the sensing orifice, that occur over much longer times, and that involve induced membrane potentials of a much smaller magnitude.

Volume regulation in the red cell is based, in part, on cation permeability, which under normal conditions is quite low. Donlon and Rothstein (1969) found that increasing the membrane potential by altering the chloride gradient leads to a monotonic increase in cation permeability. They demonstrated the existence of two regions of successively increasing slope in the graph of permeabilities vs. membrane potential: one at 45 mV and another at 180 mV. Above the higher potential, the permeability was seen to increase very rapidly. From Sale and Hamilton (1968) we calculated that an applied field of as little as 0.4 kV/cm is sufficient to induce a 180 mV membrane potential ($V_{memb} = 1.5 \times a \times E$, where a is the radius of the cell along the axis parallel to the electric field).

In the example we presented in Fig. 5, the ghosts disappeared most dramatically for the field of ~7 kV/cm. From Kachel (1979, graph, p. 69), we see that for such a field, the region of electric field strength ≥0.4 kV/cm extends several orifice diameters out from the entrance to the orifice. Because the velocity of the fluid approaching the orifice is inversely proportional to the square of the distance to the entrance (Kachel and Menke, 1979), we suggest that the time of exposure to biologically significant electrical fields may be much longer than previously thought.

Disappearing Ghosts. The preceding discussion provides the foundation for understanding the phenomenon of disappearing ghosts. We propose that at the highest field strengths, and at slow flow rates, there was sufficient time in the electric field, prior to sensing, for critically swollen ghosts to undergo a second, colloidally driven rehemolysis. In support of this idea, we found that ghosts only disappeared at slow flow, not at the faster flow rates (S. P. Akeson and H. C. Mel, unpublished data) where the exposure time before entering the sensing orifice was much shorter.

We can summarize our proposal as follows. Before entering the orifice, all the neonate ghosts in solution had resealed, while still containing some residual hemoglobin. As they approached the high-field region around the orifice and began to increase in (electrically induced) permeability, the population bifurcated. Those ghosts that could tolerate the increased colloidal osmotic pressure remained intact, and those that could not, underwent a second hemolysis. The implicit assumption is that rehemolysis under these conditions will lead to an essentially complete exchange of the remaining ghost contents with the external medium. It is very likely that, following the expulsion of the bulk of the cell's initial hemoglobin, the previously membrane-bound (residual) hemoglobin would reequilibrate to the new bulk cytoplasm. When dielectric breakdown subsequently occurred, this second class of ghosts, i.e., those that had hemolyzed for the second time, ended up with the same resistivity as the suspending medium. Such objects, being transparent to the sensing process, thus appeared to have vanished.

We may now compare the kinetics of disappearance (Fig. 5) with the kinetics of the changes in ghost resistivity (Fig. 4). The initial increase in susceptibility to disappearance at the highest field strength in Fig. 5 was paralleled by the initial rapid drop in ghost resistivity. A reasonable explanation for this observation is that both changes may reflect the basic kinetics of hemoglobin release. Furthermore, these occur at the same time (~25 s) that the neonate ghost shows maximal mechanical weakness (Yee and Mel, 1978*a*; Akeson and Mel, 1982). The longer-term change in ghost susceptibility to high fields (Fig. 5) is suggestive of a continuing, long-term action of high electric fields on cells and ghosts (work in progress).

The two concepts of the stability of volume of a post–dielectric-breakdown cell, and the disappearance of ghosts at high electric fields may at first sight appear contradictory. However, the disappearing ghosts should not be taken as evidence of volume changes of significant magnitude. These ghosts are already sphered (note the constant low-field ghost volume from 150 s onward, Fig. 3); as Jacobs and Parpart (1931) pointed out, it takes only a 0.1% increase in the cell diameter to cause an additional 5% lysis, for such critically swollen cells.

CONCLUSIONS

Electrical sizing of membrane-bounded particles at high fields provides a significantly different class of information, beyond simple volume and shape information. By coupling appropriate data taken at low electric field strengths with the data taken at high field strengths, it was possible to derive resistivities for particles during and following dielectric breakdown. The values obtained for red blood cells show an asymptotic convergence to a resistivity approximating that of the cytoplasm, for whatever cell or ghost was being probed. The technique was general enough to apply to cells having rapidly changing resistivities, objects whose resistivities would be difficult to follow by other methods.

The present studies on ghosts have demonstrated a second, important point of general interest in electronic cell sizing. Interaction of the particles with the external electric field appeared to commence at much lower field strengths than have previously been generally thought. This in turn extended the interaction with the sensing orifice much further in distance, and hence longer in time, than previously thought. While for the usual sensing fields this effect will not occur, at the highest sensing fields this electrical interaction can itself significantly alter the cells.

We would like to thank Gary Richieri for his contributions in discussions and laboratory experiments, and Dr. T. Tenforde for his timely and helpful criticisms of this manuscript.

In the early stages, this work was supported by the Director, Office of Energy Research, Office of Health and Environmental Research of the U. S. Department of Energy under contract No. DE-AC03-76SF00098.

Received for publication 14 September 1982 and in final form 2 March 1983.

REFERENCES

Akeson, S. P. 1982. Rheological and electrical properties of red blood cells and their ghosts. Ph.D. Dissertation, University of California, Berkeley, CA.

Akeson, S. P., and H. C. Mel. 1982. Osmotic hemolysis and fragility: a new model based on membrane disruption, and a potential clinical test. *Biochim. Biophys. Acta.* 718:201–211.

Anderson, P. C., and R. E. Lovrien. 1977. Human red cell hemolysis in the subsecond to seconds range. *Biophys. J.* 20:181–191.

Brecher, G., E. F. Jakobek, M. A. Schneiderman, G. Z. Williams, and P. J. Schmidt. 1962. Size distribution of erythrocytes. *Ann. NY Acad. Sci.* 99:242–261.

Coulter, W. H. 1956. High speed automatic blood cell counter and cell size analyzer. *Proc. Natl. Electron. Conf.* 12:1034–1040.

Dodge, J. T., C. Mitchell, and D. J. Hanahan. 1963. The preparation and chemical characteristics of hemoglobin-free ghosts of human erythrocytes. *Arch. Biochem. Biophys.* 100:119–130.

Donlon, J. A. and A. Rothstein. 1969. The cation permeability of erythrocytes in low ionic strength media of various tonicities. *J. Membr. Biol.* 1:37–52.

Fricke, H. 1924. A mathematical treatment of the electrical conductivity and capacity of disperse systems. *Phys. Rev.* 24:575–587.

Grover, N. B., J. Naaman, S. Ben-Sasson, and F. Doljanski. 1969. Electrical sizing of particles in suspensions. I. Theory. *Biophys. J.* 9:1398–1414.

Groves, M. R. 1980. Application of the electrical sizing principle of Coulter to a new multiparameter system. *IEEE (Inst. Electr. Electron. Eng.) Trans. Biomed. Eng.* BME-27:364–369.

Jacobs, M. H., and A. K. Parpart. 1931. Osmotic properties of the erythrocyte. II. The influence of pH, temperature, and oxygen tension on the hemolysis by hypotonic solutions. *Biol. Bull. (Woods Hole).* 60:95–119.

Jelisch, E., and U. Zimmermann. 1979. Particles in a homogeneous electrical field: a model for the electrical breakdown of living cells in a Coulter counter. *Bioelectrochem. Bioenerg.* 6:349–384.

Kachel, V. 1976. Basic principles of electrical sizing of cells and particles and their realization in the new instrument "Metricell." *J.Histochem. Cytochem.* 24:211–230.

Kachel, V. 1979. Electrical resistance pulse sizing (Coulter sizing). *In* Flow Cytometry and Sorting. M. R. Melamed, P. F. Mullaney, and M. L. Mendelsohn, editors. John Wiley & Sons, Inc., New York. 61–104.

Kachel, V., and E. Menke. 1979. Hydrodynamic properties of flow cytometric instruments. *In* Flow Cytometry and Sorting. M. R. Melamed, P. F. Mullaney, and M. L. Mendelsohn, editors. John Wiley & Sons, Inc., New York. 41–59.

Kinosita, K., and T. Y. Tsong. 1977*a*. Voltage-induced pore formation and hemolysis of human erythrocytes. *Biochim. Biophys. Acta.* 471:227–242.

Kinosita, K., and T. Y. Tsong. 1977*b*. Formation and resealing of pores of controlled sizes in human erythrocyte membrane. *Nature (Lond.).* 268:438–441.

Kinosita, K., and T. Y. Tsong. 1977*c*. Hemolysis of human erythrocytes by a transient electric field. *Proc. Natl. Acad. Sci. USA.* 74:1923–1927.

Kinosita, K., and T. Y. Tsong. 1979. Voltage-induced conductance in human erythrocyte membranes. *Biochim. Biophys. Acta.* 554:479–497.

MacGregor, R. D., and C. A. Tobias. 1972. Molecular sieving of red cell membranes during gradual osmotic hemolysis. *J. Membr. Biol.* 10:345–356.

Maxwell, J. C. 1954. Treatise on Electricity and Magnetism, Third ed. Dover Publicatios, Inc., New York, 1:437.

Mel, H. C., and T. A. Reed. 1981. Biophysical responses of red cell-membrane systems to very low concentrations of inorganic mercury. *Cell Biophys.* 3:233–250.

Pauly, H. and H. P. Schwann. 1966. Dielectric properties and ion mobility in erythrocytes. *Biophys. J.* 6:621–639.

Richieri, G. V., S. P. Akeson, and H. C. Mel. 1983. Red cell form, volume, and deformability: theory and experiment. *Biophys. J.* 41(2, Pt. 2):218*a*. (Abstr.)

Sale, A. J. H., and W. A. Hamilton. 1968. Effects of high electric fields on micro-organisms. III. Lysis of erythrocytes and protoplasts. *Biochim. Biophys Acta.* 163:37–43.

Velick, S., and M. Gorin. 1940. The electrical conductance of suspensions of ellipsoids and its relation to the study of avian erythrocytes. *J. Gen. Physiol.* 23:753–771.

Yee, J. P., and H. C. Mel. 1978*a*. Cell-membrane and rheological mechanisms: dynamic osmotic hemolysis of human erythrocytes and repair of ghosts, as studied by resistive pulse spectroscopy. *Biorheology.* 15:321–339.

Yee, J. P., and H. C. Mel. 1978*b*. Kinetics of glutaraldehyde fixation of erythrocytes: size, deformability, form, osmotic and hemolytic properties. *Blood Cells.* 4:485–497.

Zimmermann, U., G. Pilwat, and F. Riemann. 1974. Dielectric breakdown of cell membranes. *Biophys. J.* 14:881–899.

Zimmermann, U., G. Pilwat, F. Beckers, and F. Riemann. 1976*a*. Effects of external electrical fields on cell membranes. *Bioelectrochem. Bioenerg.* 3:58–63.

Zimmermann, U., G. Pilwat, Chr. Holzapfel, and K. Rosenheck. 1976*b*. Electrical hemolysis of human and bovine red blood cells. *J. Memb. Biol.* 30:135–152.

Zimmermann, U., G. Pilwat, and M. Groves. 1980*a*. Method of and apparatus for determining the breakdown characteristics of membrane-sheathed particles such as cells. U. S. patent No. 4 220 916. Granted September 1980.

Zimmermann, U., M. Groves, H. Schnabl, and G. Pilwat. 1980*b*. Development of a new Coulter counter system: measurement of the volume, internal conductivity, and dielectric breakdown voltage of a single guard cell protoplast of Vicia faba. *J. Memb. Biol.* 52:37–50.